

P-wave dibaryon resonances in pp elastic scattering and near-threshold pion production

O.A. Rubtsova,^{*} V.I. Kukulin,[†] and M.N. Platonova[‡]

Skobeltsyn Institute of Nuclear Physics, Lomonosov Moscow State University, Leninskie Gory 1/2, 119991 Moscow, Russia

(Dated: December 21, 2020)

It is demonstrated within the dibaryon-induced model for NN interaction that pp scattering in P waves is governed mainly by the production of the intermediate dibaryon resonances. Two dibaryon resonances with a mass of about 2200 MeV discovered recently by the ANKE-COSY Collaboration are shown to determine both elastic pp phase shifts and inelasticities in the 3P_0 and $^3P_2-^3F_2$ channels from zero energy up to $T_p = 0.7-0.9$ GeV. It is also demonstrated clearly that the 3P_0 dibaryon plays a decisive role in near-threshold neutral pion production in pp collisions which is poorly understood to date. The missing dibaryon contribution is found to be the very possible reason for the failure of traditional approaches to explain near-threshold π^0 production.

PACS numbers:

I. INTRODUCTION

Meson production in NN collisions is a long-standing problem in nuclear physics because such processes include rather high momentum transfers and thus the production mechanism is tightly interrelated to short-range NN dynamics which is poorly understood to date. One of the most challenging processes in this area has been the neutral pion production in pp collisions near threshold. Thus, in the early attempts to describe this process, a surprising result was attained, i.e., the theoretical cross section was found to underestimate the respective experimental data by about 5 times [1–3].

On the other hand, in the 1990ies and later, rather accurate and complete data on the near-threshold total cross section [3–5] as well as the polarisation observables [6] in the $pp \rightarrow pp\pi^0$ reaction appeared. In the experiments [6], scattering of a spin-polarised beam off a spin-polarised target was measured. The new high-precision data stimulated numerous calculations in this area (see reviews [7, 8]). The calculations within the phenomenological models (see, e.g., [9–14]) supposed various model-dependent explanations for the observed discrepancies, such as heavy meson exchanges or off-shell corrections to the πN amplitude, and were therefore inconclusive. Then the substantial progress in treating pion production was achieved within the Chiral Perturbation Theory (ChPT) [15–17] indicating that some sizable contributions to the $pp \rightarrow pp\pi^0$ cross section can come from the next-to-next-to-leading order terms of the chiral perturbation series. However, a quantitative description of neutral pion production has not been obtained to date.

It seems that the true reason for the above discrepancies was that the conventional mechanisms used to describe the data did not include some important ingredi-

ents. Thus, in Fig. 1 the direct production mechanism is shown. The pion rescattering term is small here, because, contrary to the charged pion production, the intermediate Δ contribution is suppressed due to conservation laws. In fact, for the diagrams shown in Fig. 1, there is a strong mismatch in the NN relative momenta in the initial and final states, so that, the pion production operator should include the high-momentum components. This means high sensitivity of the respective matrix elements to the πNN vertex form factor and especially to the short-range cutoff parameter $\Lambda_{\pi NN}$. It

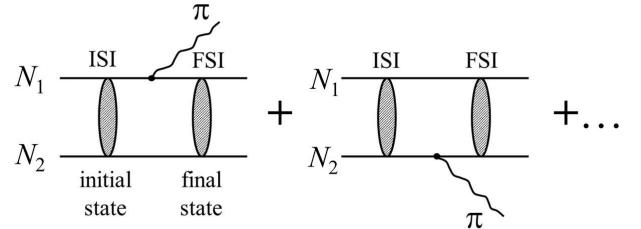


FIG. 1: The direct one-nucleon mechanism for near-threshold pion production in NN collisions.

is known that in the conventional meson-exchange approaches to the NN interaction potential, the value of $\Lambda_{\pi NN}$ is usually taken rather high, i.e., $\Lambda_{\pi NN} \simeq 1-1.7$ GeV/c (like in the Bonn family of NN potentials [18]), and the same high values of this parameter are used for the meson-exchange currents as well as for the NN wavefunctions employed for the initial state interaction (ISI) and final state interaction (FSI) treatment. Contrary to this, all microscopic meson-nucleon dynamics including $\pi N \rightarrow \Delta \rightarrow \pi N$ on-mass-shell scattering employs much lower values of the cutoff parameters, i.e., $\Lambda_{\pi NN} \simeq 0.5-0.9$ GeV/c and $\Lambda_{\pi N\Delta} \simeq 0.3-0.4$ GeV/c [19, 20]. The soft cutoff values are also consistent with the lattice-QCD calculations [21]. It is evident that an artificial increase of these parameters by 2–3 times leads immediately to the strong enhancement of the pion produc-

^{*}Electronic address: rubtsova-olga@yandex.ru

[†]Electronic address: kukulin@nucl-th.sinp.msu.ru

[‡]Electronic address: platonova@nucl-th.sinp.msu.ru

tion cross sections. We should emphasize in this regard that just the high cutoff values probably explain the success of some phenomenological models in describing near-threshold neutral pion production. E.g., the authors of Ref. [9] achieved good agreement with experimental data on the near-threshold $pp \rightarrow pp\pi^0$ cross section by introducing the short-range axial exchange charge operator with $\Lambda_{\pi NN} = 1.3$ GeV/ c taken from the Bonn NN potential.

However, when the physically justified (soft) values for the cutoff parameters are chosen, the proposed short-range contributions get considerably reduced and the meson production cross sections, in particular, in the near-threshold region, turn out to be strongly underestimated. Moreover, there are conceptual questions about the heavy meson exchange contributions (analogous to the contact terms in ChPT) which should dominate the neutral pion production near threshold as proposed in, e.g., Refs. [9, 10, 13]. From the modern viewpoint, t -channel exchange of a meson heavier than the pion between the isolated nucleons at the distances less than the nucleon size is a pure phenomenology not relevant to the real physical picture [22]. The most doubtful point seems the concept of scalar meson exchange, since the lightest scalar (σ) meson is a very broad resonance which cannot be effectively exchanged between the nucleons. The detailed discussion of these conceptual issues can be found in, e.g., [23].

So, we propose here an alternative short-range mechanism of the NN interaction which is also relevant for pion production. In view of the above arguments, it seems natural to take into account the formation of the intermediate dibaryon resonances in pp collisions, which effectively increase the meson production cross sections due to the long lifetime of the resonances. The relatively long-lived dibaryon states are produced largely due to the effect of hidden color suggested by Brodsky et al. in 1980ies [24] which prevents the resonance decay into hadronic channels. In our case, the effect of hidden color is evident when the $4q-2q$ quark-cluster model for dibaryons is used (see Sect. V of the present paper). It is important for the whole our approach that a number of dibaryon resonances in NN system have been discovered to date (see the recent review [25]).

A good illustration to these points can be found in the charged pion production process $pp \rightarrow d\pi^+$ at intermediate energies. In the conventional approaches, this process is dominated by the pion rescattering term with the Δ -isobar excitation in the intermediate state, while the direct production mechanism analogous to that shown in Fig. 1 gives only a small background. However the intermediate Δ excitation turns out to be strongly sensitive to the short-range cutoff parameters $\Lambda_{\pi NN}$ and especially $\Lambda_{\pi N\Delta}$. As we have shown in Refs. [26, 27], the above conventional mechanisms with the soft cutoff parameters consistent with πN elastic scattering give only a half cross section of the $pp \rightarrow d\pi^+$ reaction in two dominat-

ing partial waves¹ 1D_2p and 3F_3d at $T_p = 400$ –800 MeV. Nevertheless, it was demonstrated [26, 27] that one can still employ quite moderate meson-baryon cutoffs for the accurate description of this process at intermediate energies, however a non-conventional short-range mechanism for pion production should be introduced. In this novel mechanism, the basic NN interaction at short distances is driven by generation of intermediate dibaryon resonances in respective partial waves [28, 29] and thus pions are emitted from the decay of the intermediate dibaryon resonance state which drives the interaction in the given NN partial-wave channel. Thus, when the excitation of the known isovector dibaryon resonances² $^1D_2(2150)$ and $^3F_3(2220)$ near the $N\Delta$ threshold (in S and P waves, respectively) is added coherently to the t -channel Δ excitation, we achieve a very good description of the partial cross sections in the respective channels [26, 27].

The situation is even more crucial for P -wave pp scattering with the pion emitted in d wave (the 3P_2d partial channel). Here we have an analogy with the near-threshold π^0 production, where the contributions of both direct and rescattering mechanisms are strongly suppressed. In this channel, the conventional mechanisms give only a minor (ca. 2.5%) contribution which is only moderately dependent on the cutoff parameters. On the other hand, the accurate description of just the 3P_2d amplitude is crucial for reproducing the experimental data on the polarisation observables like A_{xx} , A_{yy} , etc., in $pp \rightarrow d\pi^+$ reaction. Hence, the contribution of the P -wave dibaryon $^3P_2(2200)$ (which is located also near the $N\Delta$ threshold in the relative P -wave) appears to be the *dominant one* in the 3P_2d partial channel and is clearly necessary for reproducing the polarisation observables near the resonance peak energies $T_p \simeq 600$ MeV. In Fig. 2 the partial cross section in this channel is shown in comparison with the partial-wave analysis (PWA) of the SAID group [30, 31]. It is very important that the 3P_2 dibaryon parameters found from the analysis of the $pp \rightarrow d\pi^+$ reaction turned out to be very close to those found in a recent experiment of the ANKE-COSY Collaboration [32] on a similar reaction $pp \rightarrow \{pp\}_s\pi^0$, where $\{pp\}_s$ is a near-threshold diproton in the 1S_0 state.

A quite similar situation takes place also for the isoscalar double-pion production reactions $pn \rightarrow d(\pi\pi)_0$ [26, 33]. For now, this is the most bright example of meson production through excitation of intermediate dibaryons, namely, the $d^*(2380)$ resonance discovered in a series of experiments of the WASA-at-COSY Collaboration [25]. While the energies for the d^* ex-

¹ We use here the standard notation $^{2S+1}L_Jl$ for the partial-wave channels of the $pp \rightarrow d\pi^+$ reaction, where S , L and J denote the spin, orbital and total angular momenta of the initial NN system, while l denotes the orbital angular momentum of the final pion.

² Here and below we denote the dibaryon states according to the NN channel $^{2S+1}L_J$ to which it may couple.

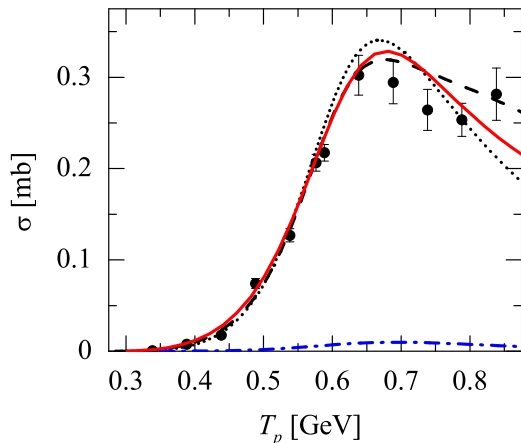


FIG. 2: Partial cross section of the reaction $pp \rightarrow d\pi^+$ in the 3P_2d channel. Shown are the summed contribution of two conventional mechanisms — pion rescattering with the intermediate Δ excitation and direct one-nucleon exchange (dash-dotted curve), the full calculation including an intermediate dibaryon formation with parameters $M({}^3P_2) = 2211$ MeV, $\Gamma({}^3P_2) = 195$ MeV (solid curve) and the SAID PWA solutions [30, 31]: C500 (dashed curve), SP96 (dotted curve) and single-energy data (filled circles).

citation in pn collisions $T_p \simeq 1.1$ – 1.2 GeV are higher than the double-pion production threshold, some interesting near-threshold phenomenon known as the ABC effect [34] also takes place here in a sense that the ABC enhancement is located near the threshold of the dipion invariant-mass spectrum [25]. In Ref. [33] we interpreted this enhancement as being due to the scalar sigma-meson production with the mass close to $2m_\pi$, which is emitted from the d^* dibaryon and then decays into two final pions. This interpretation finds support in the measured isospin dependence of the isoscalar dipion production in pn collisions [35, 36]. On the other hand, it is generally accepted that the near-threshold dipion production in NN collisions at energies $T_N < 1$ GeV goes mainly through the excitation of the intermediate Roper resonance $N^*(1440)$ [37]. However it was shown recently [38, 39] that the formation of the dibaryon resonance located near the $NN^*(1440)$ excitation threshold $\sqrt{s} \simeq 2300$ MeV (corresponding to $T_N \simeq 900$ MeV) is the most likely mechanism for both single- and double-pion production in the S -wave NN collisions. Following these lines, one could suggest the dibaryon resonances located near (almost) all nucleonic resonance thresholds to be responsible for the large portion of the meson production processes which are poorly reproduced by conventional theoretical models, especially near the respective production thresholds. For instance, the puzzling near-threshold η -meson production in pp and pd collisions (see, e.g., [40]) might be explained by the intermediate dibaryon excitation near the threshold of $NN^*(1535)$. Some experimental indications of this dibaryon have already been obtained [41, 42].

It has been shown further in Refs. [23, 38, 43, 44] that the dibaryon generation mechanism supplemented by the peripheral one-pion exchange gives an accurate description of NN phase shifts and inelasticities in various partial channels in a broad energy range from zero to about 1 GeV (lab.) and also leads to the dibaryon resonance states with parameters very close to their experimental values. The most prominent effect is seen in the 3D_3 – 3G_3 coupled channels where the decisive role of the known $d^*(2380)$ dibaryon has been shown at all energies until $T_N \simeq 1.25$ GeV [44].

In the present study we consider NN scattering in the 3P_0 , 3P_1 and 3P_2 – 3F_2 partial-wave channels. In two of these channels, viz., 3P_0 and 3P_2 , the diproton resonances with a mass of about 2200 MeV have been found in the recent experiment of the ANKE-COSY Collaboration [32] (the 3P_2 resonance was also predicted in the PWA [30, 45]). Here we study the impact of these P -wave dibaryons on both elastic and inelastic pp scattering, with a special emphasis on the near-threshold neutral pion production which is governed mainly by the 3P_0 pp initial state.

We especially emphasize here that *we do not introduce the dibaryon resonances ad hoc* to describe the particular meson production processes but instead we use the recent experimental data [32] on the P -wave dibaryons and the model developed in the earlier work [23, 38, 43, 44] which describes NN scattering at intermediate energies to analyse near-threshold pion production in pp collisions. Thus, our main goal is to reveal a connection between the NN interaction and fundamental QCD, and neutral pion production near threshold may be considered as an illustration of our general approach.

It should be also noted that the near-threshold charged pion production with the isoscalar np pair (or the deuteron) in the final state goes mainly via the 3P_1 pp collisions. However, the experimental situation with the 3P_1 dibaryon is not quite clear for now. In particular, it is not seen as a clear resonance in the respective partial channel of pp elastic scattering or the $pp \rightarrow d\pi^+$ reaction and cannot be excited at all in the $pp \rightarrow \{pp\}_0\pi^0$ process due to the angular momentum and parity conservation [32]. However, some indications of its existence can be found in the literature (see, e.g., Refs. [46–49]). Thus, for consistency of our study of P -wave pp scattering within the dibaryon model, we present below the results of calculations for the 3P_1 partial channel as well.

The structure of the paper is as follows. In Sect. II, we outline the basic formalism of the dibaryon-induced model for NN interaction and its extension for treatment of inelastic processes. In Sect. III, we present the results of the calculations for the pp elastic scattering phase shifts and inelasticities in the P -wave partial channels. In Sect. IV, we discuss in detail the near-threshold neutral pion production within the framework of the dibaryon model. Sect. V is dedicated to the feasible microscopic structure of the P -wave dibaryon resonances. Sect. VI summarizes the basic results of the present work.

II. DIBARYON-INDUCED MODEL FOR NN INTERACTION

A. Basic formalism of the model

In the dibaryon model [23, 38, 43, 44], the total Hilbert space includes two channels: an external channel corresponding to the relative motion of two nucleons and an additional internal channel which describes the formation of the six-quark (or dibaryon) state. In the simplest case, the internal space is one-dimensional, and a single internal state is associated with the “bare dibaryon” having the energy E_D .

The external Hamiltonian is represented as a sum of three terms:

$$h_{NN} = h_{NN}^0 + V_{\text{OPEP}} + V_{\text{orth}}, \quad (1)$$

where h_{NN}^0 is the two-nucleon kinetic energy operator, V_{OPEP} is the one-pion exchange potential which determines the peripheral interaction of two nucleons, and V_{orth} is an orthogonalizing potential needed to exclude the fully symmetric six-quark component from the internal state wavefunction (see below).

Here we use the same form and the same parameters of V_{OPEP} as in Refs. [23, 44]:

$$V_{\text{OPEP}} = -\frac{f_\pi^2}{m_\pi^2} (\boldsymbol{\tau}_1 \cdot \boldsymbol{\tau}_2) \frac{(\boldsymbol{\sigma}_1 \cdot \mathbf{q})(\boldsymbol{\sigma}_2 \cdot \mathbf{q})}{q^2 + m_\pi^2} \left(\frac{\Lambda_{\pi NN}^2 - m_\pi^2}{\Lambda_{\pi NN}^2 + q^2} \right)^2. \quad (2)$$

In the calculations below, we employ the soft cutoff value $\Lambda_{\pi NN} = 0.65$ GeV/c [23, 44]. This value is consistent with the microscopic quark-model [19, 20] and the lattice-QCD [21] calculations, as well as with the values commonly used in calculations of pion production (see [26] and references therein).

The potential V_{orth} has the separable form

$$V_{\text{orth}} = \lambda_0 |\phi_0\rangle\langle\phi_0|. \quad (3)$$

This term corresponds to an effective repulsion and reflects the six-quark symmetry requirements. In particular, the total microscopic six-quark wavefunctions for the S -wave NN interaction include two different (mutually orthogonal) six-quark Young schemes: $|s^6[6]\rangle$ and $|s^4p^2[42]\rangle$ in the quark shell model language. It was shown in a number of works (see, e.g., [50]) that while the fully symmetric component $|s^6[6]\rangle$ describes a bag-like structure with the hidden-color components, the mixed-symmetry component $|s^4p^2[42]\rangle$ is projected mainly onto the NN channel. So that, to exclude the non-clustered bag-like component $|s^6[6]\rangle$ from the NN relative-motion wavefunctions, one employs the orthogonalising projection operator $\lambda_0 |\phi_0\rangle\langle\phi_0|$ with a large constant λ_0 [51]. This orthogonalisation of the physical NN channel to the fully space-symmetric six-quark channel immediately leads to the nodal NN radial wavefunctions in the lower partial waves with a stable radial node against change of the collision energy [52]. It was argued in Ref. [38] that

the coupling constant λ_0 should be finite for the S -wave NN interaction to take into account the strong coupling between NN and $NN^*(1440)$ channels near the Roper resonance $N^*(1440)$ excitation threshold. On the other hand, the term (3) leads to an appearance of some excited states in the total six-quark system.

After excluding the internal channel by the standard projection technique (see details in Refs. [23, 44]), one gets an effective Hamiltonian in the NN channel with the main attraction given by the energy-dependent pole-like interaction $V_D(E)$:

$$H_{\text{eff}}(E) = h_{NN} + V_D(E), \quad V_D(E) = \frac{\lambda^2}{E - E_D} |\phi\rangle\langle\phi|, \quad (4)$$

where λ is a strength of coupling between the external and internal channels and $|\phi\rangle$ is a transition form factor. According to the symmetry requirements, the radial parts of the form factors $|\phi_0\rangle$ and $|\phi\rangle$ are taken as the lowest and the first excited harmonic oscillator wavefunctions for the given orbital angular momentum L and the same effective range r_0 :

$$\phi_0^L(k) = \sqrt{\frac{2r_0(kr_0)^{2L+2}}{\Gamma(L + \frac{3}{2})}} e^{-\frac{1}{2}(kr_0)^2}, \quad (5)$$

$$\phi^L(k) = \sqrt{\frac{2r_0(kr_0)^{2L+2}}{\Gamma(L + \frac{5}{2})}} \left[L + \frac{3}{2} - (kr_0)^2 \right] e^{-\frac{1}{2}(kr_0)^2}, \quad (6)$$

where $\Gamma(L + \frac{3}{2})$ and $\Gamma(L + \frac{5}{2})$ are the Gamma-functions. In principle, these form factors can be found from the microscopic calculations within the six-quark models as it was done, e.g., in Refs. [28, 29]. However the full and consistent six-quark calculations are still beyond our capabilities, so that, we have to consider the scale parameters r_0 of the form factors and also the coupling constants λ and λ_0 as adjustable parameters fitted to the data. Nevertheless, we tried to keep these parameter values (see Tabs. I and III) as near as possible to the six-quark model and physical estimations³.

B. Treatment of inelastic processes

In general, the internal six-quark state is able to decay into all possible inelastic (other than NN) channels, including meson and isobar production. In our model, this internal state is considered as a “bare” dibaryon resonance state. Being coupled to the NN channel, this

³ See, e.g., Ref. [29] where a direct comparison of the potential parameters found from the fit of the phase shifts with their microscopic estimations was given for the lowest NN partial channels 3S_1 – 3D_1 and 1S_0 within the initial version of the dibaryon model.

initial state gets to be additionally “dressed” by the NN loops in some analogy with the field theory.

To take into account the possible inelastic decay channels, we introduce the width Γ_{inel} for the internal state energy E_D . We suppose here the energy dependence $\Gamma_{\text{inel}}(E)$ according to the phase space of the dominant decay channel and the relative orbital angular momenta of the final particles. This dibaryon width has been introduced in our previous work [23, 44] to allow for the treatment of both elastic and inelastic NN scattering within the framework of the unified model.

Thus, the internal-state energy becomes complex-valued:

$$E_D = E_0 - i\Gamma_{\text{inel}}/2. \quad (7)$$

Generally, the width for the given decay channel can be written in the form:

$$\Gamma_{\text{inel}}(\sqrt{s}) = \begin{cases} 0, & \sqrt{s} \leq E_{\text{thr}}; \\ \Gamma_0 \frac{F(\sqrt{s})}{F(M_0)}, & \sqrt{s} > E_{\text{thr}} \end{cases}, \quad (8)$$

where \sqrt{s} is the total invariant energy of the decaying resonance, M_0 is the bare dibaryon mass related to the energy E_0 as $M_0 = 2\sqrt{m(E_0 + m)}$ (with m being the proton mass), $E_{\text{thr}} = 2m + m_\pi$ is the threshold energy and Γ_0 defines the decay width at the resonance position. The function $F(\sqrt{s})$ depends on the type of the decay process.

For the NN channels in question, the dominant decay process close to the pion production threshold should be just the emission of the neutral or charged pion, i.e., $D \rightarrow NN\pi$. The explicit expression for the function F for such a three-body decay can be taken in the following form [23]:

$$F_{NN\pi}(\sqrt{s}) = \frac{1}{s} \int_{2m}^{\sqrt{s}-m_\pi} dM_{NN} \frac{q^{2l_\pi+1} k^{2L_{NN}+1}}{(q^2 + \Lambda^2)^{l_\pi+1} (k^2 + \Lambda^2)^{L_{NN}+1}}, \quad (9)$$

where $q = \sqrt{(s - m_\pi^2 - M_{NN}^2)^2 - 4m_\pi^2 M_{NN}^2} / 2\sqrt{s}$ is the pion momentum in the total center-of-mass frame, $k = \frac{1}{2}\sqrt{M_{NN}^2 - 4m^2}$ is the momentum of the nucleon in the center-of-mass frame of the final NN subsystem with the invariant mass M_{NN} , and Λ is the high-momentum cutoff parameter which prevents an unphysical rise of the width Γ_{inel} at high energies. The orbital angular momenta of the emitted pion l_π and the nucleon in the NN subsystem L_{NN} may take different values in accordance with the total angular momentum and parity conservation. For the 3P_0 initial channel, we parameterize the dibaryon width according to the dominant near-threshold Ss final state with $L_{NN} = l_\pi = 0$, while for the 3P_2 channel we take $L_{NN} = 0$ and $l_\pi = 2$ which correspond to the final Sd configuration.

It should be noted that for the 3P_2 and 3P_1 channels, the decay process $D \rightarrow d\pi$ with the final deuteron is also important near the inelastic threshold. In such a case, the function F takes a simple form corresponding to the two-body decay:

$$F_{d\pi}(\sqrt{s}) = \frac{q^{2l_\pi+1}}{(q^2 + \Lambda_{d\pi}^2)^{l_\pi+1}}, \quad (10)$$

where q is the pion momentum and $\Lambda_{d\pi}$ is the high-momentum cutoff parameter. It can be shown that the general three-body expression (9) can be reduced to the two-body form similar to Eq. (10) in the case of small relative momenta of two emitted nucleons due to the close values of the deuteron mass m_d and the two-nucleon threshold energy $M_{NN} = 2m$. Thus, one can use the three-body parametrization of Γ_{inel} (8) for all three isovector P -wave NN channels (with the function F defined by Eq. (9)) as the most common form of the decay width which effectively takes into account the possible inelastic processes for these channels near the inelastic threshold. For the description of NN scattering phase shifts at higher energies, the energy behaviour of the dibaryon decay width is much less important, so that, Eq. (9) can be used to represent the width also above the threshold region.

The bare dibaryon mass M_0 and width Γ_0 are renormalised in the course of dressing by the NN loops, i.e., when solving the scattering equations with the effective Hamiltonian (4), thus resulting in the “dressed” dibaryon mass M_{th} and width Γ_{th} which can be compared to the experimental dibaryon position. The inelastic width at the resonance point $\Gamma_{\text{inel}}(M_{\text{th}})$ determines the coupling of the dibaryon resonance in question to the inelastic channels, the main one being the $NN\pi$ channel. Accordingly, the elastic decay width of the dibaryon can be found as $\Gamma(D \rightarrow NN) = \Gamma_{\text{th}} - \Gamma_{\text{inel}}(M_{\text{th}})$ (see details in Ref. [23]).

III. DESCRIPTION OF pp SCATTERING IN P WAVES

A. Partial phase shifts and inelasticities in the channels 3P_0 and 3P_2 - 3F_2

Below we consider the results of calculations using the above formalism for the pp partial-wave channel 3P_0 and the coupled channels 3P_2 - 3F_2 . The parameters of the model used in the present calculations are listed in Tab. I. Here a single internal state for the coupled channels 3P_2 and 3F_2 is introduced (see the details below). The mass m_π has been taken to be equal to the neutral pion mass. The main parameters of the P -wave dibaryon resonances in the effective Hamiltonian (4), i.e., the mass M_0 and width Γ_0 of the bare resonance, have been fitted to reproduce the partial phase shifts and inelasticity parameters in a broad energy interval up to the resonance positions for the given NN channels.

TABLE I: Parameters of the dibaryon model potential for the NN partial-wave channels 3P_0 and 3P_2 - 3F_2 .

	λ_0	r_0	λ	M_0	Γ_0
	MeV	fm	MeV	MeV	MeV
3P_0	450	0.425	35	2200	92
3P_2	0	0.7	63	2205	100
3F_2	105	0.45	1.5		

With these model parameters, one gets the “dressed” resonance states in both configurations with the masses M_{th} and widths Γ_{th} shown in Tab. II. We emphasise that these values occur to be fully consistent with the experimental ones found in Ref. [32].⁴ So, these two basic parameters of the dibaryon resonances in our model can be fixed by the experimental data.

TABLE II: Comparison of the experimental values for the resonance masses and decay widths with those found in the dibaryon model for the NN partial-wave channels 3P_0 and 3P_2 - 3F_2 .

	M_{th}	Γ_{th}	M_{exp}	Γ_{exp}
	MeV	MeV	MeV	MeV
3P_0	2200	99	2201(5)	91(12)
3P_2 - 3F_2	2221	168	2197(8)	130(21)

Using Eqs. (8), (9) and the values of the dibaryon mass and width given in Tab. II, one can estimate the branching ratio for the dibaryon decay into the NN channel: $\text{BR}(D \rightarrow NN) = (\Gamma_{\text{th}} - \Gamma_{\text{inel}}(M_{\text{th}}))/\Gamma_{\text{th}}$ [23]. Thus, we obtain this branching ratio to be about 7% and 13% for the 3P_0 and 3P_2 - 3F_2 dibaryons, respectively. These values are consistent with the value of 10% obtained for the P -wave dibaryons from the PWA of pp scattering [46, 47]. So, these dibaryons are highly inelastic as well as other known dibaryons above the pion production threshold [25].

1. The channel 3P_0

The partial phase shifts for the pp channel 3P_0 are displayed in Fig. 3 in comparison with the PWA results of the SAID group [31].

As is clearly seen from the Figure, we have achieved almost perfect agreement with the results of PWA in a very broad energy range from zero energy to about 1 GeV. To make the result more evident, we have also shown on Fig. 3 the phase shifts corresponding to the pure OPEP (dashed curve). This comparison makes clear the fact that the dibaryon formation in our model provides the

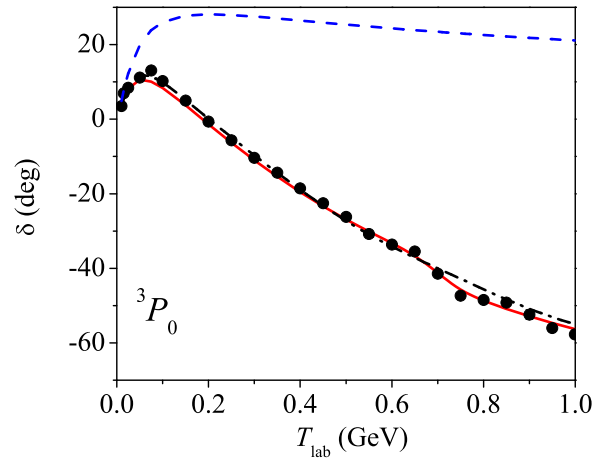


FIG. 3: (Color online) Partial phase shifts for the pp channel 3P_0 found within the dibaryon model (solid curve) in comparison with the single-energy SAID PWA [31] (filled circles), the SAID SM16 solution [31] (dash-dotted curve) and results for the pure OPEP (dashed curve).

dominant part of the NN interaction in the whole energy region considered.

To take an effective account of inelastic processes, we have used here Eqs. (8) and (9) for the internal state decay width corresponding to the single-pion production. The resulted inelasticity parameters are shown in Fig. 4. Again, a very good agreement with the PWA results is seen up to the energies near the resonance position. Further, the total inelasticity continues to increase signaling about other inelastic processes (such as double-pion production, etc.) while the inelasticity predicted by the dibaryon model decreases.

We emphasize here that the excellent description of both elastic phase shifts and inelasticities shown in Figs. 3 and 4 has been attained using the same pole parameters, i.e., within a unified model.

2. The coupled channels 3P_2 - 3F_2

The preliminary study of the NN scattering phase shifts and inelasticity parameters in the 3P_2 channel within the dibaryon model has already been published in Ref. [23]. Here they are explored in a more detail with inclusion of coupling with the 3F_2 channel and focusing on the description of inelastic processes. Due to account of the PF coupling, the dibaryon part of the interaction in Eq. (4) should have the following form:

$$V_D(E) = \frac{1}{E - E_D} |\Phi\rangle\langle\Phi|, \quad |\Phi\rangle = \begin{pmatrix} \lambda_P |\phi_P\rangle \\ \lambda_F |\phi_F\rangle \end{pmatrix}, \quad (11)$$

where $|\Phi\rangle$ contains two form factors corresponding to coupling of the internal state with two partial NN chan-

⁴ The F -wave admixture to the 3P_2 state was not considered in the experimental work [32].

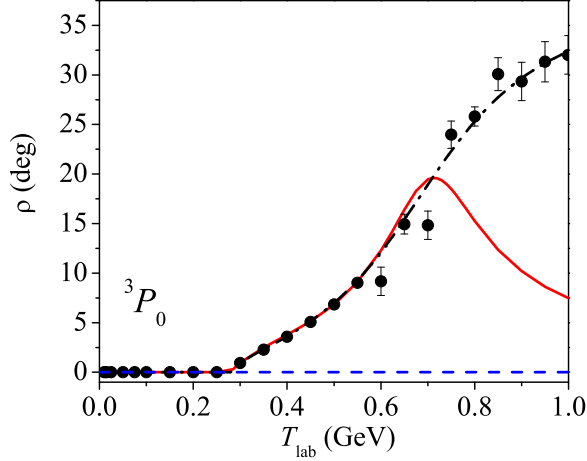


FIG. 4: (Color online) Inelasticity parameters for the pp channel 3P_0 found within the dibaryon model (solid curve) in comparison with the single-energy SAID PWA [31] (filled circles), SAID SM16 solution [31] (dash-dotted curve) and results for the pure OPEP (dashed curve).

nels in question. Eq. (11) results in the following matrix form of the interaction:

$$V_D(E) = \frac{1}{E - E_D} \begin{pmatrix} \lambda_P^2 |\phi_P\rangle\langle\phi_P| & \lambda_{PF}^2 |\phi_P\rangle\langle\phi_F| \\ \lambda_{PF}^2 |\phi_F\rangle\langle\phi_P| & \lambda_F^2 |\phi_F\rangle\langle\phi_F| \end{pmatrix}, \quad (12)$$

where $\lambda_{PF} = \sqrt{\lambda_P \lambda_F}$ and the non-diagonal parts give impact to the tensor component of the total interaction.

In Eq. (11), the partial form factors are taken again as the harmonic oscillator functions corresponding to the orbital angular momentum L and the effective range r_0 . However, in contrast to the 3P_0 channel, the 3P_2 partial phase shifts are positive and do not show any repulsion until the energy of about 1 GeV. Hence, the orthogonalizing potential is needed in the F -wave channel only. So that, the form factor $|\phi_P\rangle$ represents the lowest harmonic oscillator wavefunction given by Eq. (5) with $L = 1$, while the form factors $|\phi_0\rangle$ and $|\phi_F\rangle$ represent the lowest and the first excited harmonic oscillator functions defined in Eqs. (5) and (5), respectively, with $L = 3$. The model parameters for these coupled channels are collected in Tab. I.

The 3P_2 and 3F_2 pp scattering phase shifts and the mixing angle ε_2 are shown in Fig. 5 in comparison with the SAID PWA [31] and the pure OPEP contribution. It is seen that the phase shift 3F_2 is represented quite well up to 1 GeV. However, the good description of the partial phase shifts in the 3P_2 channel is obtained until ca. 700 MeV (i.e., up to the resonance position) only. The coupling between the P and F waves is small here which results in a rather small mixing angle. As is seen from Fig. 5c, this mixing angle is defined essentially by the tensor part of the OPEP. At the same time, the tensor part

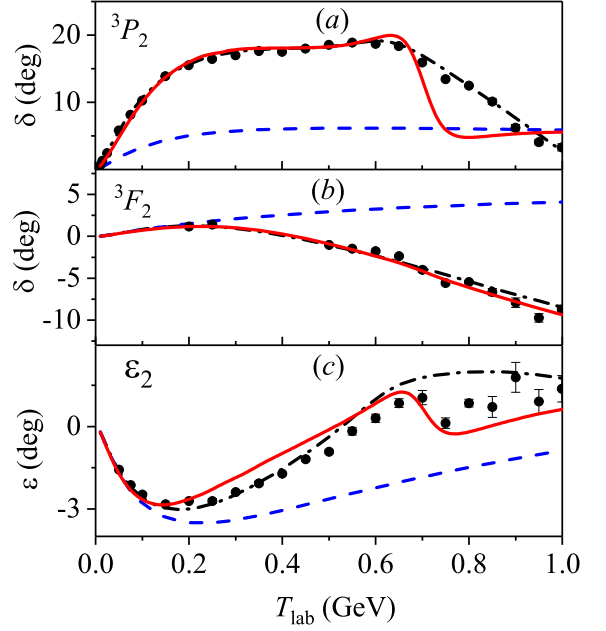


FIG. 5: (Color online) Partial phase shifts for the coupled pp channels 3P_2 (a) and 3F_2 (b) and the mixing angle ε_2 (c). The notations are the same as in Fig. 3.

of the dibaryon potential gives the required correction near the resonance position. However, its contribution turns out to be slightly overestimated in the intermediate energy region.

The respective inelasticity parameters found within the dibaryon model are shown in Fig. 6. Although some overestimation of the inelasticity is seen in 3P_2 channel in the intermediate energy region, one can get a reasonable average description of the inelastic processes in both P and F partial waves.

To summarize the comparison with the PWA data, it should be emphasized that a rather simple form of the interaction with a single internal state allows us to reproduce quite well *all five scattering parameters* (i.e., the phase shifts, the inelasticities and mixing angles) corresponding to the coupled NN channels 3P_2 - 3F_2 and simultaneously gives the resonance position (see Tab. II) which is very close to the experimental one [32]. At the same time, some deviations from the PWA results are seen which should stimulate some further improvements of the model.

In particular, small discrepancies between our calculations and the PWA data in the near-threshold region might be explained by the more involved structure of the dibaryon decay width in the 3P_2 channel compared to the 3P_0 one, where the final Ss configuration dominates the near-threshold pion production. For the 3P_2 initial channel, the Sd , Ds and Pp final configurations can give comparable contributions, while we take into account the Sd configuration only (which is appropriate for the $d\pi^+$

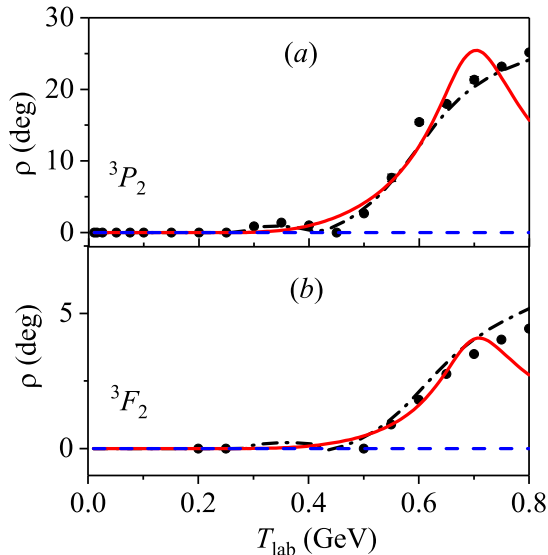


FIG. 6: (Color online) Inelasticity parameters for the coupled pp channels 3P_2 (a) and 3F_2 (b). The notations are the same as in Fig. 4.

final state). Thus, the correct description of the total inelasticities in the 3P_2 – 3F_2 partial channels requires a detailed dynamical model for the dibaryon decay in various final states instead of our simple width parametrization. Such a dynamical description of all dibaryon decay channels is beyond the scope of the present work.

B. Partial phase shifts and inelasticities in the channel 3P_1

For consistency of our study of the P -wave pp scattering within the dibaryon model, we should examine the model in the 3P_1 partial channel as well. Though the 3P_1 dibaryon resonance has not been detected in experiments to date, different estimations from the PWA of pp scattering can be found in the literature. In particular, in Ref. [46], the resonance state with the mass $M(^3P_1) = 2179$ MeV and the width $\Gamma(^3P_1) = 86$ MeV was found from the PWA of pp scattering. At the same time, the hypothetical 3P_1 dibaryon state with the mass $M(^3P_1) \simeq 2.07$ GeV can be considered as a member of the Regge trajectory for isovector dibaryons [48]. The resonance with the same mass was also mentioned in Ref. [49].

Below we show the results of the calculations of the 3P_1 pp phase shifts within the dibaryon model for one of the possible parameter sets (see Tab. III). Here, the effective range r_0 of the dibaryon part of the interaction is the same as for the channel 3P_0 (see Tab. I).

The partial phase shifts and inelasticity parameters for the channel 3P_1 are shown in Figs. 7 and 8, respectively,

TABLE III: Parameters of the dibaryon model potential for the NN partial-wave channel 3P_1 .

	λ_0	r_0	λ	M_0	Γ_0
	MeV	fm	MeV	MeV	MeV
3P_1	270	0.425	20	2230	50

in comparison with the SAID PWA data. Similarly to the 3P_0 case, one obtains the good description of these quantities up to laboratory energies of about 1 GeV. More-

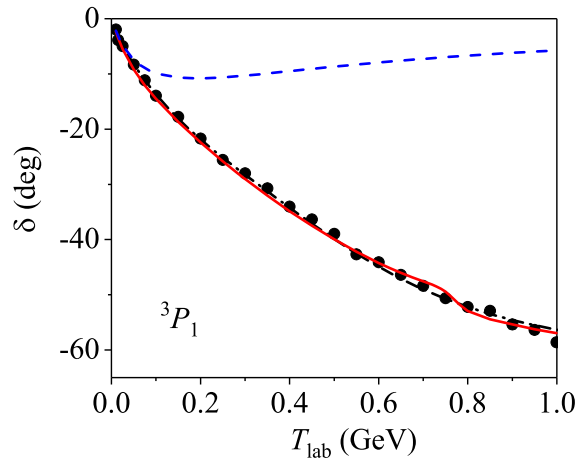


FIG. 7: (Color online) Partial phase shifts for the pp channel 3P_1 . The notations are the same as in Fig. 3.

over, with the parameters chosen, the model allows us to reproduce the peak that appears in the SAID single-energy data near $T_{\text{lab}} = 0.75$ GeV. It should be noted however, that the energy-dependent SAID solution does not reveal such a peak.

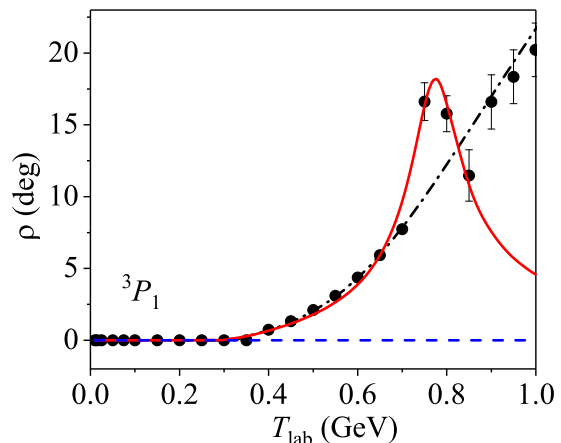


FIG. 8: (Color online) Inelasticity parameters for the pp channel 3P_1 . The notations are the same as in Fig. 4.

Finally, the suggested dibaryon potential results in the “dressed” dibaryon resonance with the mass $M_{\text{th}}(^3P_1) = 2230$ MeV and the width $\Gamma_{\text{th}}(^3P_1) = 52.5$ MeV. Thus, the total width of the 3P_1 dibaryon in our model turns out to be narrower than those for other P -wave dibaryons. For the branching ratio of the 3P_1 dibaryon decay into the NN channel we obtain the value of about 5% which is somewhat smaller than for the other P -wave dibaryons as well. We should note however, that the parameters of the model potential and the resulted dibaryon resonance which allow us to describe reasonably pp scattering in the 3P_1 channel are not unique. So, additional support from the experimental side is needed to draw unambiguous conclusions about the existence of the 3P_1 dibaryon.

IV. DESCRIPTION OF NEAR-THRESHOLD NEUTRAL PION PRODUCTION

In Sect. III A above, we have shown within the dibaryon model that the resonance $^3P_0(2200)$ found clearly in the experiment [32] determines the pp inelasticity in the 3P_0 channel from the inelastic threshold to about $T_{\text{lab}} = 700$ MeV. In turn, the near-threshold inelasticity here is mainly due to the neutral pion production, since the process $pp \rightarrow pp\pi^0$ in the near-threshold region is by far dominated by the 3P_0 initial state of the pp pair which is coupled to the 1S_0 pp final state with an s -wave emitted pion (the so-called Ss partial amplitude) [5].⁵ On the other hand, the total inelastic pp cross section in the 3P_0 channel consists of two parts corresponding to the above neutral pion production process and also the charged pion production reaction $pp \rightarrow pn\pi^+$. Due to the different dynamics of these processes, including the different final state interaction of the pp and np pairs with the small relative momenta, it seems nontrivial to extract these amplitudes separately. However, the threshold of the charged pion production is shifted by about 10 MeV (in the lab. energy) from that of the neutral pion production. Thus, one has a unique situation in the small energy interval just above the neutral pion production threshold, where the total cross section of the $pp \rightarrow pp\pi^0$ reaction should closely coincide with the total inelastic cross section in the pp partial channel 3P_0 . Thus, the dibaryon resonance which governs pp scattering in the 3P_0 channel, should determine also near-threshold π^0 production in pp collisions.

The proposed dibaryon mechanism for near-threshold π^0 production is depicted in Fig. 9.

The fundamental difference between the traditional mechanism for the π^0 production displayed in Fig. 1 and the dibaryon-induced mechanism for this process shown

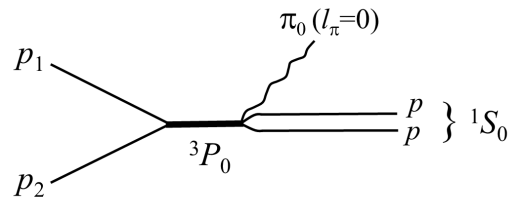


FIG. 9: The dibaryon-induced mechanism for near-threshold π^0 production in the 3P_0 pp channel which leads to the 1S_0 pp final state. The microscopic interpretation of the production mechanism in terms of the $4q$ - $2q$ six-quark model is presented in Sect. V.

in Fig. 9 is as follows. The dominating NN channel leading to the π^0 near-threshold production is 3P_0 which is odd with respect to the two-nucleon permutation. So that, for the single-nucleon contributions to the π^0 production from the 3P_0 initial channel of the type shown in Fig. 1 a strong mutual cancellation between the production on the first and second nucleons takes place, while the dibaryon mechanism shown in Fig. 9 has no such mutual single-particle cancellation.

In Fig. 10 we compare the total inelastic cross section found for the 3P_0 channel within our model with the existing experimental data for the near-threshold π^0 production [3, 4].

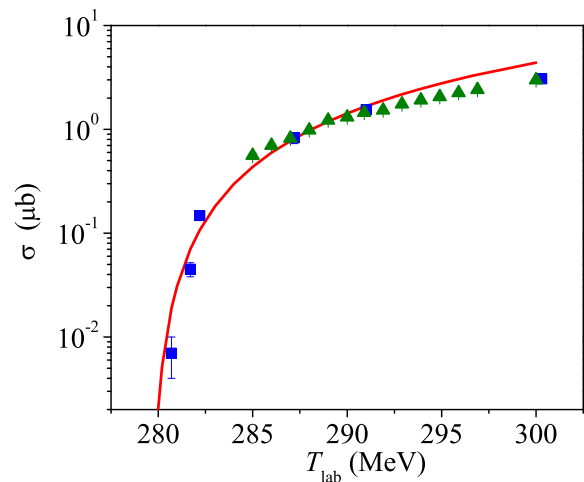


FIG. 10: (Color online) The total inelastic pp cross section in the 3P_0 channel found within the dibaryon model (solid curve) in comparison with experimental data on the total $pp \rightarrow pp\pi^0$ cross section from Refs. [3] (triangles) and [4] (squares).

Very good agreement between our calculations and experimental data is seen in the energy interval $T_p = 280$ – 290 MeV just above the neutral pion production threshold. It should be emphasized that although some small discrepancies with the data are visible in some experi-

⁵ For the initial pp pair in the 3P_0 state, there is also a small admixture of the 3P_1p (or Pp) final configuration which is rising with the collision energy [5].

mental points, the general behavior of the cross section as a function of the collision energy is reproduced quite well. On the one hand, it is not surprising to have a good description of the near-threshold π^0 production provided the total inelasticity of pp scattering is fitted in the 3P_0 channel. On the other hand, it was not evident at all that a simple model with a single dibaryon pole located rather far from the πNN threshold could reproduce the pp inelasticity in a broad energy range, including a very good description of the near-threshold region. At higher energies, above the charged-pion production threshold, the total inelastic pp cross section overestimates the experimental data on the neutral pion production, due to the rising contribution of the process $pp \rightarrow pn\pi^+$.

It has been demonstrated already in Ref. [3] that the qualitative behavior of the near-threshold neutral pion production cross section can be understood in terms of the three-body phase space multiplied by a FSI factor. On the other hand, in the current version of the dibaryon model, an account of inelastic processes is done by incorporating the decay width Γ_{inel} . Thus, the success of the model in the description of the near-threshold pion production cross section is due to the proper behaviour of the function (9) at small pion momenta q . For the Ss channel, this function indeed behaves as a three-body phase space with a cutoff factor, which effectively takes into account the FSI between the final protons. However, our results are more general since this width parametrization allows us to reproduce the pp inelasticity not only near the pion production threshold but in a wide energy interval up to the dibaryon resonance position.

Thus, within the model suggested, we have a good description of pp elastic scattering in the 3P_0 partial channel from zero energy up to about 1 GeV and the correct near-threshold behaviour of the neutral pion production cross section as well. We can conclude therefore that pp scattering in this channel is determined almost completely by the 3P_0 dibaryon resonance with a mass of about 2200 MeV.

The 3P_2 pp channel also plays an important role in the neutral pion production process [32]. However, the respective amplitude is small in the near-threshold region due to the angular momentum barrier. At the same time, at energies where it becomes larger, our theoretical total inelastic amplitude includes effectively not only the $pp\pi^0$ channel but also $pn\pi^+$ and $d\pi^+$ ones. Thus, we cannot extract the contribution of the 3P_2 dibaryon to the particular inelastic processes within the current version of the model. However, we have got a reasonable description of the elastic phase shift and the total inelasticity in the 3P_2 channel as well. Besides that, our study of the reaction $pp \rightarrow d\pi^+$ by inclusion the dibaryon resonances into the leading partial-wave amplitudes has shown the dominance of the 3P_2 dibaryon in the respective partial cross section (see Ref. [27] and Fig. 2 of the present paper). These results allow us to suppose the leading role of the dibaryon mechanism in pp elastic scattering and pion production processes in the 3P_2 channel from threshold

up to the resonance position.

Finally, the 3P_1 dibaryon, if it exists, should determine the near-threshold charged pion production processes in pp collisions with the isoscalar np (or the deuteron) final state, i.e., $pp \rightarrow \{pn\}_{I=0}\pi^+$ and $pp \rightarrow d\pi^+$. However, it is non-trivial to separate these processes with the very near thresholds having just the total inelastic cross section in the 3P_1 channel. So, we restrict ourselves to the reasonable description of the scattering phase shift and the total inelasticity in this channel as well.

V. MICROSCOPIC STRUCTURE OF P -WAVE DIBARYON RESONANCES

In the previous section, we demonstrated that the 3P_0 and 3P_2 isovector dibaryon resonances discovered recently by the ANKE-COSY Collaboration [32] govern both NN elastic and inelastic scattering in the respective partial-wave channels from zero energy until at least 700 MeV. We have also shown that the near-threshold production of neutral pions is determined mainly by the 3P_0 dibaryon resonance.

On the other hand, we discussed in Ref. [26] some possible realisation of the Nijmegen-ITEP quark-cluster model [53, 54] for the well-known isovector dibaryon resonance trajectory 1D_2 , 3F_3 , 1G_4 , etc. The feasible realisation of the general $4q$ - $2q$ model for the straight-line isovector dibaryon trajectory is the six-quark structure shown in Fig. 11. Here S and T are the spin and isospin of the tetraquark $4q$ while the respective values for the diquark $2q$ are denoted as S' and T' .

In the six-quark model proposed here, i.e., with $ST = 01$ and $S'T' = 00$, the total angular momentum is equal to the orbital angular momentum, i.e., $J = L$, and the total isospin $T_{\text{tot}} = 1$. In this way, we can describe the whole isovector trajectory 1S_0 , 3P_1 , 1D_2 , 3F_3 , 1G_4 , etc., considered in Ref. [48] as rotational excitations in the NN system, by a rotating color string between the $4q$ and $2q$ clusters with the orbital angular momenta $L = 0, 1, 2, \dots$, respectively.⁶ Most of these isovector dibaryons have been detected to date, except for the 3P_1 resonance which should have the mass of about 2.07 GeV to fit into the above trajectory [48]. On the other hand, in the present study we have obtained the 3P_1 dibaryon resonance with the mass $M_{\text{th}}(^3P_1) = 2230$ MeV, i.e., close to the 3P_0 and 3P_2 resonances found experimentally. So, one can suppose that the 3P_1 resonance is shifted somehow by the spin-orbital forces which mix three P -wave states with different J , or, alternatively, that there are

⁶ Note that in Ref. [26] the quantum numbers ST and $S'T'$ were selected in a different way which did not allow for a description of two lowest members of the isovector dibaryon trajectory, i.e., 1S_0 and 3P_1 . The 3P_0 and 3P_2 resonances also did not fit into that classification, so the three-diquark structure was suggested for them in Ref. [27].

two 3P_1 dibaryons separated by about 150 MeV. However, since no one of these resonances has been detected to date, we restrict the following consideration to the 3P_0 and 3P_2 states.

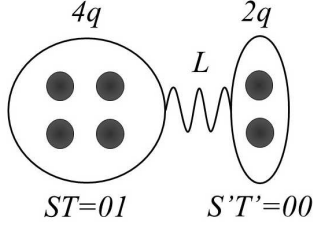


FIG. 11: The tetraquark-diquark model for the dibaryon state with the colour string connecting two quark clusters.

Then the important question arises, i.e., could the microscopic structure within the framework of the above $4q-2q$ model be relevant also for the isovector dibaryon resonances 3P_0 and 3P_2 ? In fact, one can suggest for the 3P_0 and 3P_2 states a similar $4q-2q$ microscopic structure but now with $ST = 01$, $S'T' = 11$ and $L = 1$. This corresponds to the plausible quantum numbers of the $6q$ state, i.e., $S_{\text{tot}} = 1$, $T_{\text{tot}} = 1$ and $J = L \pm 1 = 0, 2$. In such a case, two P -wave dibaryons 3P_0 and 3P_2 should have just the $N-\Delta$ hadronic structure with the relative P wave between the nucleon and the Δ -isobar. So, we have here an analogy with the structure of the well-known ${}^1D_2(2150)$ dibaryon lying very near to the $N-\Delta$ threshold with a relative S -wave between N and Δ .

Assuming further the above $4q-2q$ structure for the 3P_0 and 3P_2 dibaryons (with $ST = 01$, $S'T' = 11$ and $L = 1$), one may explain the π^0 emission from these dibaryons leading to a final 1S_0 diproton as a two-step process:

$$pp \rightarrow D({}^3P_{J=0,2}) \rightarrow \{pp\}_s + \pi^0|_{l_\pi=0,2}. \quad (13)$$

This process goes through a conventional quark spin-isospin flip inside the axial-vector diquark: $S'T' = 11 \rightarrow 00$, with an accompanying deexcitation of the colour string $L = 1 \rightarrow 0$ to compensate the parity change in the pion emission with $l_\pi = 0$ or 2 .

Thus, the suggested six-quark picture gives at least a qualitative explanation for the pion emission induced by the intermediate 3P_0 and 3P_2 dibaryons.

VI. CONCLUSION

In the present work, we studied the impact of the recently discovered [32] P -wave dibaryon resonances with a

mass of about 2200 MeV on pp elastic scattering and pion production in pp collisions. Within the dibaryon-induced model for NN interaction, we have demonstrated that these P -wave dibaryons give a quite reasonable description of the pp scattering phase shifts and inelasticities in the 3P_0 and ${}^3P_2-{}^3F_2$ partial channels from zero energy to at least 700 MeV (lab.). Furthermore, we have shown that the 3P_0 dibaryon resonance determines almost completely the neutral pion production process $pp \rightarrow \{pp\}_s \pi^0$ in the near-threshold region. It should be stressed that the respective cross section does not find a satisfactory explanation within the conventional approaches. So, within the dibaryon model proposed, the amplitude of near-threshold π^0 production in pp collisions is reproduced consistently with the pp elastic scattering amplitudes in the above partial-wave channels. The 3P_2 dibaryon resonance also gives an important contribution to both neutral and charged pion production in a broad energy range, though its contribution is suppressed near threshold by the angular momentum barrier.

We have also achieved a very good description of the pp scattering phase shift and inelasticity in the 3P_1 partial channel at $T_{\text{lab}} = 0-700$ MeV, using the dibaryon with a mass $M({}^3P_1) = 2230$ MeV, i.e., rather close to that of the 3P_0 and 3P_2 resonances found experimentally [32]. If this dibaryon exists, it should determine the charged pion production processes $pp \rightarrow d\pi^+$ and $pp \rightarrow \{pn\}_{I=0} \pi^+$ near threshold. In fact, it seems natural to have three almost degenerate P -wave dibaryons with $J = 0, 1, 2$ coupled with the spin-orbit force. It should be borne in mind however, that the 3P_1 dibaryon has not been detected to date, though some indications of its existence can be found in the literature. So, an additional experimental confirmation of these results is needed.

The results of the present work should be considered jointly with our previous conclusions [27] about dominance of the 3P_2 dibaryon resonance in the charged pion production process $pp \rightarrow d\pi^+$ in the 3P_2d partial wave and the crucial role of the dibaryon in the proper description of polarization observables in this process. A good description of both neutral and charged pion production as well as NN elastic scattering within the unified dibaryon model gives a strong argument in favour of the decisive role of dibaryon resonances in NN collisions at intermediate energies in general.

Acknowledgments. The work has been partially supported by RFBR, grants Nos. 19-02-00011, 19-02-00014. M.N.P. also appreciates support from the Foundation for the Advancement of Theoretical Physics and Mathematics “BASIS”.

[1] D.S. Koltun, A. Reitan, Phys. Rev. **141**, 1413 (1966).

[2] G.A. Miller, P.U. Sauer, Phys. Rev. C **44**, R1725 (1991).

- [3] H.O. Meyer *et al.*, Nucl. Phys. A **539**, 633 (1992).
- [4] A. Bondar *et al.*, Phys. Lett. B **356**, 8 (1995).
- [5] R. Bilger *et al.*, Nucl. Phys. A **693**, 633 (2001).
- [6] H.O. Meyer *et al.*, Phys. Rev. Lett. **81**, 3096 (1998); H.O. Meyer *et al.*, Phys. Rev. Lett. **83**, 5439 (1999); P. Thörnngren-Engblom *et al.*, Nucl. Phys. A **663**, 447c (2000); P. Thörnngren-Engblom *et al.*, arXiv: nucl-ex/9810013 (1998).
- [7] C. Hanhart, Phys. Rept. **397**, 155 (2004).
- [8] V. Baru, C. Hanhart, F. Myhrer, Int. J. Mod. Phys. E **23**, 1430004 (2014).
- [9] T.-S.H. Lee and D.O. Riska, Phys. Rev. Lett. **70**, 2237 (1993).
- [10] C.J. Horowitz, H.O. Meyer, D.K. Griegel, Phys. Rev. C **49**, 1337 (1994).
- [11] V.P. Andreiev *et al.*, Phys. Rev. C **50**, 15 (1994).
- [12] C. Hanhart, J. Haidenbauer, O. Krehl, J. Speth, Phys. Lett. B **444**, 25 (1998); Phys. Rev. C **61**, 064008 (2000).
- [13] V. Malafaia, M.T. Peña, Ch. Elster, J. Adam Jr., Phys. Rev. C **74**, 042201(R) (2006).
- [14] E. Hernandez and E. Oset, Phys. Lett. B **350**, 158 (1995).
- [15] B.-Y. Park, F. Myhrer, J.R. Morones, T. Meissner and K. Kubodera, Phys. Rev. C **53**, 1519 (1996).
- [16] C. Hanhart and N. Kaiser, Phys. Rev. C **66**, 054005 (2002).
- [17] A.A. Filin *et al.*, Phys. Rev. C **85**, 054001 (2012); *ibid.* **88**, 064003 (2013); A.A. Filin *et al.*, EPJ Web Conf. **81**, 03003 (2014); V. Baru *et al.*, Eur. Phys. J. A **52**, 146 (2016).
- [18] R. Machleidt, K. Holinde, Ch. Elster, Phys. Rep. **149**, 1 (1987); R. Machleidt, Phys. Rev. C **63**, 024001 (2001).
- [19] W. Koepf, L.L. Frankfurt, and M. Strikman, Phys. Rev. D **53**, 2586 (1996).
- [20] J. Flender and M.F. Gari, Phys. Rev. C **51**, R1619 (1995).
- [21] K.F. Liu *et al.*, Phys. Rev. D **59**, 112001 (1999); G. Erkol, M. Oka, and T.T. Takahashi, Phys. Rev. D **79**, 074509 (2009).
- [22] T. Barnes, S. Capstick, M.D. Kovarik, and E.S. Swanson, Phys. Rev. C **48**, 539 (1993).
- [23] V.I. Kukulin, V.N. Pomerantsev, O.A. Rubtsova, M.N. Platonova, Phys. At. Nucl. **82**, 934 (2019).
- [24] S.J. Brodsky, C.-R. Ji, and G.P. Lepage, Phys. Rev. Lett. **51**, 83 (1983); S.J. Brodsky and C.-R. Ji, Phys. Rev. D **33**, 1406 (1986); M. Bashkanov, S.J. Brodsky, and H. Clement, Phys. Lett. B **727**, 438 (2013).
- [25] H. Clement, Prog. Part. Nucl. Phys. **93**, 195 (2017) and references therein.
- [26] M.N. Platonova and V.I. Kukulin, Nucl. Phys. A **946**, 117 (2016).
- [27] M.N. Platonova and V.I. Kukulin, Phys. Rev. D **94**, 054039 (2016).
- [28] V.I. Kukulin, I.T. Obukhovskiy, V.N. Pomerantsev, and A. Faessler, J. Phys. G **27**, 1851 (2001).
- [29] V.I. Kukulin, I.T. Obukhovskiy, V.N. Pomerantsev, and A. Faessler, Int. J. Mod. Phys. E **11**, 1 (2002).
- [30] C.-H. Oh, R. A. Arndt, I.I. Strakovsky, R.L. Workman, Phys. Rev. C **56**, 635 (1997).
- [31] R.L. Workman, W.J. Briscoe, and I. I. Strakovsky, Phys. Rev. C **94**, 065203 (2016); all SAID PWA solutions can be accessed via the website: <http://gwdac.phys.gwu.edu>
- [32] V. Komarov *et al.*, Phys. Rev. C **93**, 065206 (2016).
- [33] M.N. Platonova and V.I. Kukulin, Phys. Rev. C **87**, 025202 (2013).
- [34] A. Abashian, N.E. Booth, K.M. Crowe, Phys. Rev. Lett. **5**, 258 (1960); N.E. Booth, A. Abashian, K.M. Crowe, *ibid.* **7**, 35 (1961).
- [35] P. Adlarson *et al.*, Phys. Lett. B **721**, 229 (2013).
- [36] M.N. Platonova and V.I. Kukulin (to be published).
- [37] L. Alvarez-Ruso, E. Oset, E. Hernandez, Nucl. Phys. A **633**, 519 (1998).
- [38] V.I. Kukulin *et al.*, Eur. Phys. J. A **56**, 229 (2020).
- [39] H. Clement and T. Skorodko, arXiv:2010.09217 [nucl-ex].
- [40] P. Adlarson *et al.*, Phys. Lett. B **782**, 297 (2018).
- [41] T. Ishikawa *et al.*, Phys. Lett. B **789**, 413 (2019).
- [42] D. Tsirkov *et al.*, EPJ Web Conf. **199**, 02016 (2019).
- [43] V.I. Kukulin, V.N. Pomerantsev, O.A. Rubtsova, Few-Body Syst. **60**, 48 (2019).
- [44] V.I. Kukulin *et al.*, Phys. Lett. B **801**, 135146 (2020).
- [45] R.A. Arndt *et al.*, Phys. Rev. D **28**, 97 (1983); R.A. Arndt *et al.*, Phys. Rev. C **76**, 025209 (2007).
- [46] A.V. Kravtsov, M.G. Ryskin, I.I. Strakovsky, J. Phys. G **9**, L187 (1983); I.I. Strakovsky, A.V. Kravtsov, M.G. Ryskin, Sov. J. Nucl. Phys. **40**, 273 (1984).
- [47] I.I. Strakovsky, Fiz. Elem. Chastits At. Yadra **22**, 615 (1991); AIP Conf. Proc. **221**, 218 (1991).
- [48] M.H. MacGregor, Phys. Rev. D **20**, 1616 (1979).
- [49] E. Ferreira, G.A. Pérez Munguia, J. Phys. G **9**, 169 (1983).
- [50] Y. Yamanuchi, M. Wakamatsu, Nucl. Phys. A **457**, 621 (1986); A. Faessler, F. Fernandez, Phys. Lett. B **124**, 145 (1983); V.I. Kukulin, V.N. Pomerantsev, Progr. Theor. Phys. **88**, 159 (1992).
- [51] V.I. Kukulin, V.N. Pomerantsev, Ann. Phys. (N.Y.) **111**, 330 (1978).
- [52] V.I. Kukulin, V.G. Neudatchin, Yu. F. Smirnov, Phys. Elem. Chastits At. Yadra **10**, 1236 (1979).
- [53] P.J. Mulders, A.T.M. Aerts, and J.J. De Swart, Phys. Rev. D **21**, 2653 (1980).
- [54] L.A. Kondratyuk, B.V. Martemyanov, M.G. Shchepkin, Sov. J. Nucl. Phys. **45**, 776 (1987).